ELSEVIER

Journal of Organometallic Chemistry 632 (2001) 197–208

Journal of Organometallic Chemistry

www.elsevier.com/locate/jorganchem

Synthesis, bonding and dynamic behavior of *fac*-[Mo(II)(CO)$_2$(η^3-allyl)] derivatives

J.R. Ascenso [a], C.G. de Azevedo [a,*], M.J. Calhorda [b,c], M.A.A.F. de C.T. Carrondo [b], P. Costa [b], A.R. Dias [a], M.G.B. Drew [e], V. Félix [d], A.M. Galvão [a], C.C. Romão [b]

[a] *Centro de Química Estrutural, Complexo I, Instituto Superior Técnico, Av. Rovisco Pais, 1, 1049-001 Lisbon, Portugal*
[b] *Instituto de Tecnologia Química e Biológica, Av. da República, EAN, Apt 127, 2781-901 Oeiras, Portugal*
[c] *Departamento de Química e Bioquímica, FC, Universidade de Lisboa, 1749-016 Lisbon, Portugal*
[d] *Departamento de Química, Universidade de Aveiro, 3810-193 Aveiro, Portugal*
[e] *Department of Chemistry, University of Reading, Whiteknights, Reading RG6 2AD, UK*

Received 5 March 2001; accepted 10 May 2001

Abstract

Cationic complexes [Mo(η^3-allyl)(CO)$_2$(L–L)L′]PF$_6$, (L–L = $C_6H_5SCH_2CH_2SC_6H_5$, L′ = $NCCH_3$ (**1**); bipy, $NCCH_3$ (**2**); py, $(NCCH_3)_2$ (**3**); $(NCCH_3)_3$ (**4**); dppe, $NCCH_3$ (**5**) and the neutral analogues [Mo(η^3-allyl)(CO)$_2$(L–L)X] (L–L = phen (**6**); bipy (**7**); X = Br) were synthesized. Complexes **2**, **5**, **6** and **7** were characterized by single crystal X-ray diffraction. Depending on the chelating ligand, these pseudo-octahedral complexes undergo different dynamic processes in solution and NMR spectroscopic evidence was provided for those studies. The structural trends of the limiting structures depicted by these complexes as well as the pathways to their inter-conversion were analyzed by ab initio theoretical calculations. Both NMR data and the calculations showed that for complex **2** the equatorial species predominates at room temperature but that two forms differing only by the conformation of the allyl coexist. Lowering the temperature leads to the appearance of the equatorial–axial isomer.

Keywords: Molybdenum; Allylic complexes; Ab initio calculations; Dynamic NMR; X-ray diffraction

1. Introduction

There is a large number of molybdenum-η^3-allyl-carbonyl complexes of general formula [Mo(η^3-C_3H_5)-(CO)$_2$L$_2$X] and [Mo(η^3-C_3H_5)(CO)$_2$(L-L)X] in which X is either a halide or pseudohalide and L is a monodentate ligand and (L–L) a bidentate ligand [1].

These complexes have been found to act as catalysts for the polymerization of certain dienes [2a,b] (when X = CF_3 and L–L = $CH_3O(CH_2)_2OCH_3$) and the halide phosphine substituted analogues have been utilized in organic synthesis for allylic alkylations [3a–d]. Therefore, investigations have been carried out to study the factors that determine their stereochemistry, reactivity, and possible dynamic processes in solution. There are studies on the molecular orbital analysis of the regioselectivity of nucleophilic addition to η^3-allyl complexes and the relative orientation of the η^3-allyl ligand in [Mo(η^3-C_3H_5)(CO)$_2$(L–L)L′] complexes [4]. The *fac*-[Mo(η^3-C_3H_5)(CO)$_2$] moiety occurs in all η^3-allyldicarbonylmolybdenum (II) complexes so far investigated. The allylic group has its terminal C atoms eclipsing the carbonyls, which has been demonstrated to be the most energetically favorable arrangement. Stereochemical nonrigidity in molybdenum(II) π-allyl complexes has been widely studied [5] and shows that they can adopt, in the solid state, either a symmetric (A) or a non-symmetric (B) structure (Scheme 1).

Although most of the complexes whose structure has been determined adopt configuration A, and there are only few examples of structure B [3f], there seems to be no obvious reason for the choice. In solution, these complexes exhibit dynamic behavior [6] with interconversion of the two species. Several solution dynamic

* Corresponding author. Tel: +351-1-21841-9284; fax: +351-1-21846-4455/57.
E-mail address: cristina.azevedo@ist.utl.pt (C.G. de Azevedo).

0022-328X/01/$ - see front matter
PII: S0022-328X(01)00988-3

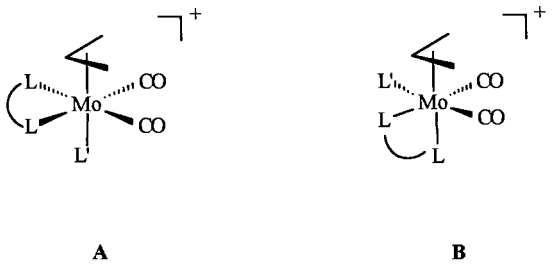

Scheme 1.

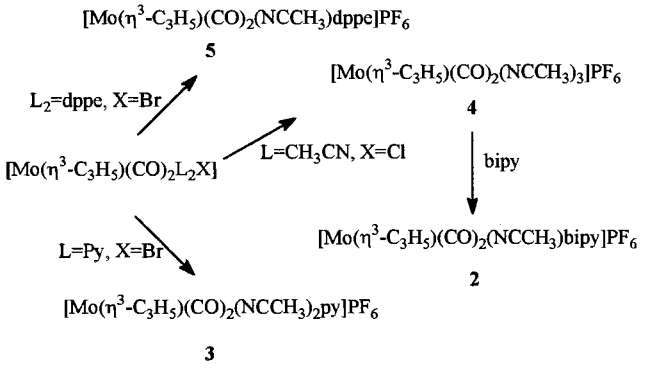

Scheme 2.

mechanisms have been proposed to account for this process: the nondissociative intramolecular trigonal-twist rearrangement [6b,7–9,10c] or turnstile mechanism [3f,11], which involves rotation of the face formed by X and L–L with respect to the face formed by the allyl and two carbonyl groups, and can retain or remove the elements of chirality. Recently a 'pivoted double switch' mechanism has been reported in which two coordination sites are scrambled causing racemisation [5]. Other solution dynamic behavior involves the allyl group (*exo*/*endo* orientation) either by rotation about the metal-π-allyl axis or via a $\eta^3-\eta^1-\eta^3$ rearrangement [3f,12,13].

The $[Mo(\eta^3\text{-}C_3H_5)(CO)_2(NCCH_3)_2X]$ complex has been extensively used for the synthesis of many allylic derivatives, which may be obtained by replacement of the weakly bonded nitriles by nitrogen [14–16], phosphorus [17], arsenic [6a], or carbocyclic [18] ligands. Although a large number of such complexes has been made, the examples reported with sulfur ligands are much rarer and they involve (*S*,*S*) anionic donors [19,20].

We wish therefore to report new Mo(II) allyl complexes of general formula $[Mo(\eta^3\text{-}C_3H_5)(CO)_2(L\text{–}L)X]$ with sulfur ligands and the cationic analogues $[Mo(\eta^3\text{-}C_3H_5)(CO)_2(L\text{–}L)L']^+$. The solid state structure of the cation **2** (L–L = bipy, L′ = $NCCH_3$) was determined at room and at low temperature, allowing the observation of the allyl geometry in great detail. It can be compared with the structure of the related complexes $[Mo(\eta^3\text{-}C_3H_5)(CO)_2(L\text{–}L)Br]$ (L = phen (**6**); bipy (**7**)), which were also determined. Molecular orbital calculations [21,22] have been carried out in order to compare the stability of the possible isomers and their interconversion mechanisms. NMR studies were performed with the aim of understanding and examining possible dynamic processes in solution.

2. Results and discussion

2.1. Chemical studies

The new complex $[Mo(\eta^3\text{-}C_3H_5)(CO)_2(PhSCH_2\text{-}CH_2SPh)]PF_6$ (**1**) can be prepared by the reaction of $[Mo(\eta^3\text{-}C_3H_5)(CO)_2(NCCH_3)_2Cl]$ with $PhSCH_2CH_2SPh$ in acetone with 50% yield, making use of the usual lability of the acetonitrile ligand. The complex is both air and thermally sensitive, and is hence stored at −20 °C.

Addition of $TlPF_6$ to a solution of $[Mo(\eta^3\text{-}C_3H_5)(CO)_2bipyBr]$ in acetonitrile gave, after refluxing, a red compound, which was identified as $[Mo(\eta^3\text{-}C_3H_5)(CO)_2bipy(NCCH_3)]PF_6$, (**2**), in 80% yield. A similar reaction using appropriate precursors gave, in refluxing acetonitrile and in the presence of $TlPF_6$, the expected $[Mo(\eta^3\text{-}C_3H_5)(CO)_2(NCCH_3)_2py]PF_6$ (**3**) and $[Mo(\eta^3\text{-}C_3H_5)(CO)_2(NCCH_3)_3]PF_6$ (**4**). The addition of one equivalent gram of dppe to a CH_2Cl_2 solution of **4** led to $[Mo(\eta^3\text{-}C_3H_5)(CO)_2(NCCH_3)dppe]PF_6$ (**5**) in 74% yield.

From the results described above it is clear that the $[Mo(\eta^3\text{-}C_3H_5)(CO)_2(L\text{–}L)X]$ complexes react with $TlPF_6$, with halide abstraction, to give, in the presence of coordinating solvent, the respective cation as shown in Scheme 2.

The type of reaction described provides an easy and general route to allyl-carbonyl cationic derivatives of general formula $[Mo(\eta^3\text{-}C_3H_5)(CO)_2(L\text{–}L)L']^+$, some of which are already known [23]. Analogous cationic Mo(II) and W(II) derivatives have been reported, namely $[Mo(\eta^3\text{-}C_3H_4R)(CO)_2(bipy)L]BF_4$ (R = H, Me; L = NH_3, py, PPh_3, $AsPh_3$, $P(PhO)_3$) [24], $[Mo(\eta^3\text{-}C_3H_4R)(CO)_2(R'N{=}CHCH{=}NR')py]^+$ (R = H, Me; R′ = Me, Et, ^{i}Pr, Ph, etc) [16] and $[Mo(\eta^3\text{-}C_3H_4R)(CO)_2(bipy)py]^+$ [25].

The IR data for **2**, **3**, **4**, **5** show two strong carbonyl bands of equal intensity, consistent with *cis*-carbonyl groups in the $[Mo(\eta^3\text{-}C_3H_5)(CO)_2]$ moiety.

NMR data at room temperature and above indicated fluxional behavior in solution for all complexes. Taking **2** as an example, the room temperature ^{1}H-NMR spectrum shows two groups of three resonances assigned to the AM_2X_2 spin system characteristic of symmetrical π-allyls and two sets of bipyridyl peaks. ^{13}C-NMR data shows two carbonyl carbon signals. The only dynamic

process consistent with this NMR data is an exchange process by allyl rotation. That the allyl motion is indeed a rotation and not a $\pi-\sigma-\pi$ rearrangement was confirmed from a series of 1D spin saturation transfer experiments. Irradiation of the *anti* protons of one isomer caused a drop in intensity of the *anti* protons of the other with no change in intensity of the *syn* protons. A symmetrically averaged spectrum is observed at high temperature (62 °C) with only one allylic and one bipyridyl pattern. This reflects the presence of two isomers (A and A′) slowly interconverting in solution, at room temperature as is shown in Scheme 3. Raising the temperature favors a faster rotation of the allyl and average spectra were observed.

Both the geometry of the isomers and the dynamic process in complex **2** were confirmed by phase sensitive 2D ^{1}H-NOESY spectra recorded at 27 °C, shown in Fig. 1.

In Fig. 1a negative cross-peaks due to chemical exchange are observed between H_{meso} of A and H_{meso} of A′, H_{syn} (A) and H_{syn} (A′) and H_{anti} (A) and H_{anti} (A′). Fig. 1b shows positive cross-peaks due to NOEs between both H_{syn} and H_{meso} (A and A′) and H_6 and $H_{6'}$ of the bipy ligand. NOEs between H_{anti} and H_6 or $H_{6'}$ were not observed. For each isomer the expected NOEs between the protons of the same allyl were detected. These NOE correlations give structural information about the molecule and indicate that the bipy is coordinated in the equatorial position in both isomers A and A′.

The low temperature ^{1}H-NMR spectrum exhibits two sets of resonances for the allyl moiety. One is typical of the A_2B_2X spin system of symmetrical η^3-allyl metal complexes. The ABCDX spin pattern observed for the other set demonstrates the magnetic non-equivalence of the methylene termini of the allyl ligand in the instantaneous structure and is characteristic of an asymmetric allylic complex. Both structures A and B (Scheme 1) are consistent with this pattern. The spectroscopic data support the coexistence in solution at low temperature of isomers A and B, corresponding to an equatorial coordination of the bipy ligand for A and an equatorial–axial geometry for B. A mechanism fully consistent with the NMR spectral data obtained can be

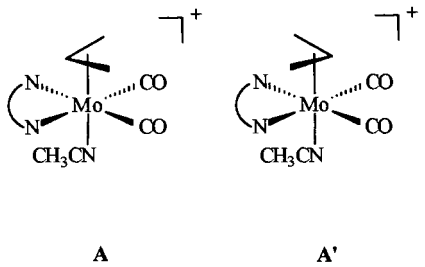

Scheme 3.

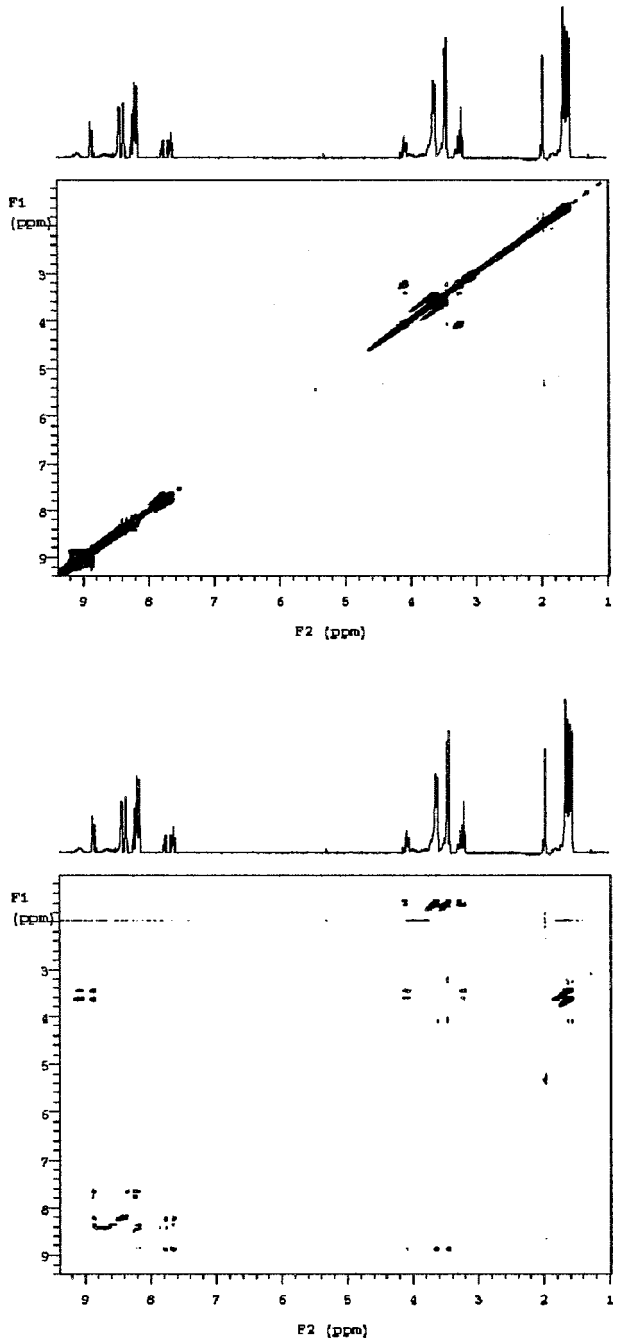

Fig. 1. Phase sensitive 2D NOESY experiment for **2** at 27 °C: (a) negative peaks related with chemical exchange of magnetization; (b) positive peaks due to NOEs.

described as the trigonal-twist. This process involves the rotation of the triangular face formed by the three nitrogen atoms with respect to the face formed by the allyl and the two carbonyl groups. The type B structure presents enantiomerization of the metal center and the rearrangement depicted in Scheme 4 illustrates a molecule interconverting between the two enantiomers.

The geometry of complex 2 and the presence of A, B and B′ were confirmed by a phase sensitive 2D ^{1}H-

NOESY spectrum recorded at −30 °C, shown in Fig. 2.

At this temperature, the proton signals have split and the interchange processes are slow. In Fig. 2a cross-peaks due to chemical exchange are observed between H_6 (B) and H_6 (B′), H_{syn} (B) and H_{syn} (B′) and H_{anti} (B) and H_{anti} (B′). These observations are consistent with a racemization process taking place for B. Fig. 2b shows positive cross-peaks from NOEs between $H_{6,6'}$ (A) and H_{syn} (A). This correlation indicates a close spatial proximity of the *syn* protons of the allyl ligand and H_6 and $H_{6'}$ of the bipy ligand. The corresponding peaks are not detected for B, which is consistent with the geometry already proposed for A and B. For each isomer the expected NOEs between the protons of the same allyl are detected. Since B and B′ are interconverting, indirect NOEs for H_{anti} (B) and H_{syn} (B′) and H_{anti} (B′) and H_{syn} (B) are also observed.

2.2. Structural studies

The solid state structures of the PF_6 salts of cationic complexes $[Mo(\eta^3\text{-allyl})(CO)_2(L{-}L)L']PF_6$, (L–L = bipy, L′ = $NCCH_3$ (**2**); dppe, $NCCH_3$ (**5**)) and the neutral analogues $[Mo(\eta^3\text{-allyl})(CO)_2(L{-}L)X]$ (L–L = phen (**6**); bipy (**7**); X = Br) were determined by single crystal X-ray diffraction at room temperature. In order to determine the positions of the hydrogen atoms of the allyl ligand with a high degree of precision, an X-ray determination of the structure of **2** at low temperature (173 K) was also carried out. This study offers the possibility of analyzing the change of the overall geometry of the allyl ligand associated with η^3-cordination, namely the bending of the two *anti* protons away from the allylic plane. Selected bond lengths and angles are given in Table 1. Molecular diagrams of the complexes **2**, **5**, **6** and **7**, showing the overall geometry and labeling scheme adopted, are recorded in Figs. 3–6, respectively. Furthermore, Fig. 3 shows an ORTEP diagram for the low temperature study.

In all complexes the cordination environment of the molybdenum center is pseudo octahedral with two carbon atoms from the carbonyl groups and the centroid of the allyl ligand determining a *fac* stereochemistry. In all structures the allyl ligand adopts the usual *endo*

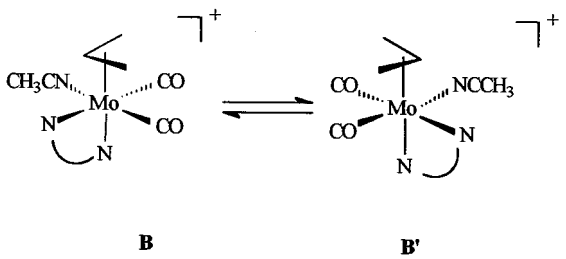

Scheme 4.

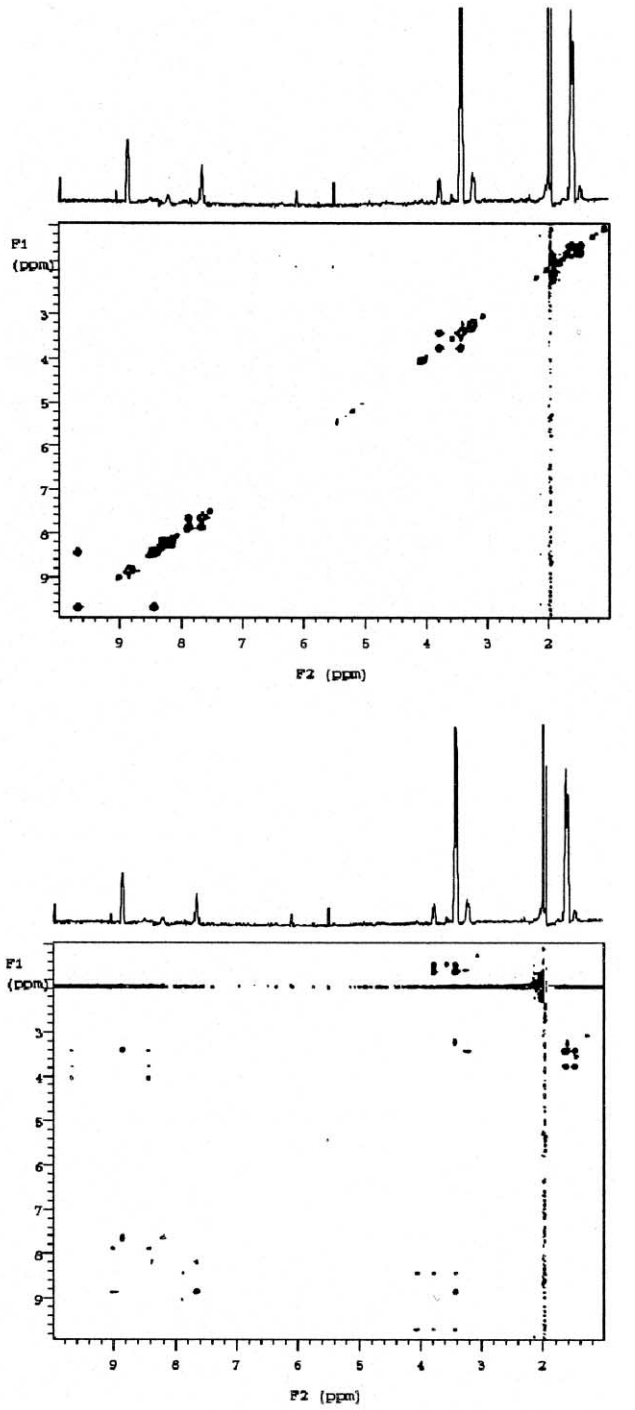

Fig. 2. Phase sensitive 2D NOESY experiment for **2** at −30 °C: (a) negative peaks related with chemical exchange of magnetization; (b) positive peaks due to NOEs.

conformation in the solid state, with the open side eclipsing the two carbonyls. The chelation of the bidentate ligands occurs in different sites of the metal coordination sphere and two different geometric arrangements are observed, as shown in Scheme 1. Thus, the two nitrogen donors from the bipy in **2** and the two phosphorus donors from the dppe in **4** occupy

Table 1
Selected bond lengths (Å) and bond angles (°) in the molybdenum coordination sphere for complexes **2**, **5**, **6** and **7**

[Mo(η³-allyl)(CO)$_2$bipy(NCCH$_3$)]$^+$ (**2**)		[Mo(η³-allyl)(CO)$_2$-dppe(NCCH$_3$)]$^+$ (**5**)		[Mo(η³-allyl)(CO)$_2$phenBr] (**6**)		[Mo(η³-allyl)(CO)$_2$bipyBr] (**7**) [a]	
Bond lengths							
Mo–C(100)	1.968(4)	Mo–C(100)	1.946(6)	Mo–C(100)	1.959(6)	Mo–C(100)	1.951(7)
Mo–N(11)	2.252(3)	Mo–N(300)	2.233(5)	Mo–N(11)	2.248(5)	Mo–Br	2.650(3)
Mo–N(300)	2.197(3)	Mo–P(7)	2.537(3)	Mo–Br	2.645(2)	Mo–N(11)	2.233(5)
Mo–C(200)	1.943(4)	Mo–C(200)	1.973(6)	Mo–C(200)	1.961(6)		
Mo–N(21)	2.213(3)	Mo–P(4)	2.602(4)	Mo–N(21)	2.269(4)		
Bond angles							
C(100)–Mo–C(200)	82.3(2)	C(100)–Mo–C(200)	78.2(2)	C(100)–Mo–C(200)	79.7(2)	C(100)*–Mo–C(100)	80.9(4)
C(100)–Mo–N(300)	172.5(1)	C(200)–Mo–N(300)	101.0(2)	C(200)–Mo–N(11)	169.1(2)	C(100)–Mo–N(11)*	167.5(2)
C(100)–Mo–N(21)	88.0(1)	C(200)–Mo–P(7)	80.8(2)	C(200)–Mo–N(21)	102.9 (2)	C(100)–Mo–N(11)	101.7(3)
N(300)–Mo–N(21)	84.5(1)	C(100)–Mo–P(4)	98.1(2)	N(11)–Mo–C(3)	119.1(2)	C(100)*–Mo–Br	85.8(2)
C(100)–Mo–N(11)	98.4(1)	N(300)–Mo–P(4)	81.8(1)	C(100)–Mo–Br	87.0(2)	C(1)–Mo–Br	149.1(2)
N(300)–Mo–N(11)	80.3(1)	C(100)–Mo–N(300)	177.7(2)	N(11)–Mo–Br	81.0(1)	O(101)–C(100)–Mo	179.2(6)
C(301)–N(300)–Mo	173.4(3)	C(100)–Mo–P(7)	94.6(2)	O(101)–C(100)–Mo	177.9(5)	C(100)*–Mo–N(11)*	101.7(3)
O(101)–C(100)–Mo	176.2(3)	N(300)–Mo–P(7)	83.1(2)	C(100)–Mo–N(11)	102.2(2)	C(100)*–Mo–N(11)	167.5(2)
C(200)–Mo–N(300)	97.1(1)	C(200)–Mo–P(4)	158.3(2)	C(100)–Mo–N(21)	169.0(2)	N(11)*–Mo–N(11)	73.2(3)
C(200)–Mo–N(21)	92.5(1)	P(7)–Mo–P(4)	78.2(1)	N(11)–Mo–N(21)	73.2(2)	C(100)–Mo–Br	85.8(2)
C(200)–Mo–N(11)	165.0(2)			N(21)–Mo–C(3)	82.1(2)	N(11)–Mo–Br	82.2(2)
N(21)–Mo–N(11)	72.6(1)			C(200)–Mo–Br	88.3(2)		
N(300)–C(301)–C(302)	179.7(5)			N(21)–Mo–Br	82.4(1)		
O(201)–C(200)–Mo	176.4(3)			O(201)–C(200)–Mo	176.9(5)		

[a] *Symmetry transformation used to generate equivalent atoms: x, $-y+1/2$, z.

an equatorial and an axial coordination position (B in Scheme 1). In both complexes, the remaining equatorial position is taken by an acetonitrile ligand. By contrast, the phen in **6** and bipy in **7** constitute together with two carbonyl groups the equatorial coordination plane (A in Scheme 1). In both complexes, the axial position *trans* to the allyl moiety is occupied by a bromine atom.

Table 2 summarizes the structural data relevant for characterizing the complexes reported here, together with the data for other related *fac*-Mo(η³-C$_3$H$_5$)(CO)$_2$ derivatives.

The two geometric arrangements found for the studied complexes can be easily characterized by Ω, which is the angle between the line defined by the centroid of the allyl moiety and the molybdenum with the Mo–X bond, X representing the donor atom from the monodentate ligand. This Ω parameter gives the orientation of the monodentate ligand relative to the allyl fragment and determines unequivocally the position of the bidentate ligand in the metal coordination sphere. Thus, in complexes **6**, **7**, **9**, **10**, **11** and **13** the bidentate ligand is on the equatorial position and values of Ω close to 180° were observed. By contrast, in complexes **2**, **5**, **8** and **12** the Ω angle takes values close to 90° and the chelation of the bidentate ligand occurs via equatorial and axial sites. Furthermore, the structural data presented in Table 2 show that there is no structural relationship between the Mo–X distance and the isomer found, since dppe complexes **8** with Mo–Cl of 2.573 Å and **5** Mo–NCCH$_3$ of 2.233(5) Å exhibit the same stereochemistry. In some octahedral complexes of type *fac*-[Mo(η³-allyl)(CO)$_2$L$_2$Br] containing other bidentate ligands, available from the Cambridge Data Base [29], the bromine is equatorial while in the others it is axial. There is no obvious structural preference.

The chelation of bipy leads to N–Mo–N angles of 72.6(1)° in **2** and 73.2(3)° in **7**, which are identical to those reported for phen of 73.2(2)° in **6**. These values are typical of coordinated polypyridinic ligands and are due to small bite angles of phen and bipy as seen for the values quoted in Table 2 for other examples. The chelation of dppe in **5** also leads to the formation of a five chelate-membered ring, but this ligand is sterically

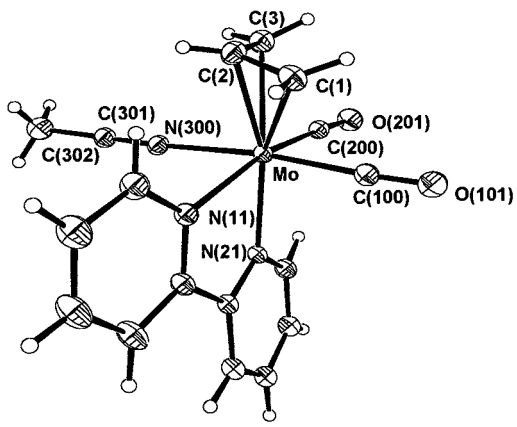

Fig. 3. The structure of [Mo(η³-allyl)(CO)$_2$bipy(NCCH$_3$)]$^+$ (**2**) with ellipsoids at 30% probability at 173 K.

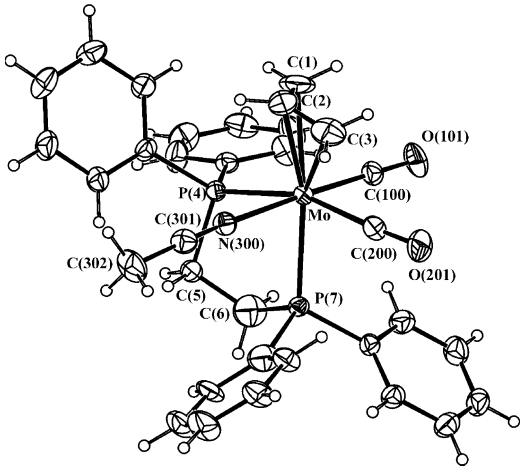

Fig. 4. The structure of $[Mo(\eta^3\text{-allyl})(CO)_2dppe(NCCH_3)]^+$ (**5**) with ellipsoids at 30% probability.

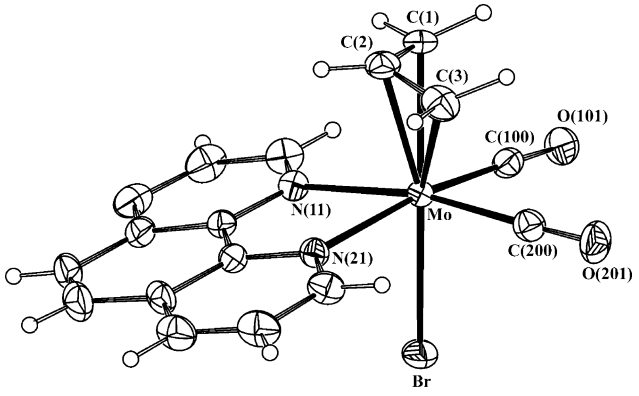

Fig. 5. The structure of $[Mo(\eta^3\text{-allyl})(CO)_2phenBr]$ (**6**) with ellipsoids at 30% probability.

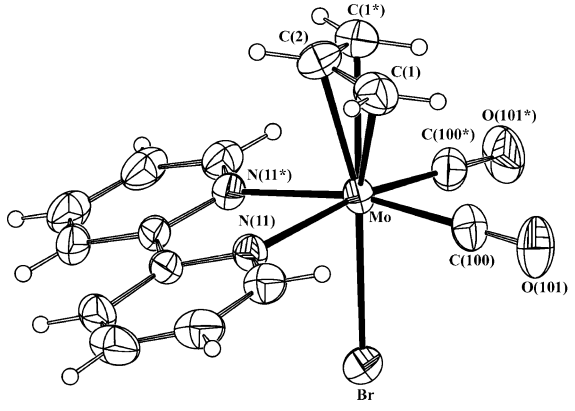

Fig. 6. The structure of $[Mo(\eta^3\text{-allyl})(CO)_2bipyBr]$ (**7**) with ellipsoids at 30% probability.

more flexible, and a wider P–Mo–P angle of 78.2(1)° was found, comparable to the angle 75.3° reported for **8**. All molecular dimensions found for the studied complexes are within the expected values.

The structure observed at low temperature for complex **2** (Fig. 3) has no significant differences in the molecular dimensions and conformation of the allyl group from that at room temperature. Nevertheless, the location and unrestricted refinement of all hydrogen positions and thermal motion parameters allow us to discuss in further detail the geometry of the allyl ligand, namely the pyramidalization of the terminal carbon atoms with the *anti* hydrogens bending away from the allylic plane (Table 3). The data at room and low temperature are comparable, although the low temperature refinement shows a large residual density (eight peaks), located at around 0.7–0.9 Å of the Mo atom, in the bisecting directions of the X–Mo–X coordination sphere. This feature may be attributed to *d* density since data at low temperature was collected up to 32° in theta. The scattering factors for higher multipole terms in charge density (d^2) are more important at higher angles and not accounted in a spherical atom refinement. Nevertheless, collecting some higher angle data allowed us to perform a valence density multipole refinement to study further the allyl electronic features. The *syn* and *anti* hydrogen atoms of the allyl bend away from the allylic plane by significant amounts, while the *meso* hydrogen remains on that plane. Similar distortions were observed in complexes **5** and **6**, where the atomic positions of the hydrogen atoms were also obtained from difference Fourier maps.

The elongated shape of the fluorine atom F(1) ellipsoid (in the counter ion) can also be explained by a double hydrogen bond to one of the $NCCH_3$ hydrogen atoms (2.48(12) Å, angle 172(11)°) and to the *anti* hydrogen of a symmetry $(-1/2+x,\ 1/2-y,\ 1/2+z)$ related molecule (2.53(8) Å, angle 154(5)°).

The low temperature data was also used in a valence density refinement which allowed us to analyze the experimental electronic density in the allyl plane (Fig. 7), where the carbon atoms and the *syn* and *meso* hydrogens can be located. An interesting feature in this map is the extra density peak originated in the metal orbitals. This peak lies in the center of a virtual pentagon containing the three carbons and two imaginary atoms and not in the geometric center of the allyl group.

2.3. Calculations

Ab initio DFT calculations (details in Section 4) were performed on several possible isomers of complex **2**, using as model $[Mo(\eta^3\text{-allyl})(CO)_2(bipy)(NCH)]^+$ where the methyl group of the nitrile was replaced by a hydrogen atom. Two limiting structures with a *fac* arrangement of the carbonyls and the geometric center of the allyl group were found (or the three nitrogen atoms). The most stable, by 2 kJ mol^{-1}, contains chelating bidentate ligand occupying one axial and one equatorial positions (B in Scheme 5), while in the next

Table 2
Structural data for *fac*-[Mo(η^3-allyl)$(CO)_2$(L–L)X]^n complexes ($n = 0$, 1)

Complex		Distances (Å)				Angles (°)			Ref.
		⟨Mo–P⟩	⟨Mo–N⟩	Mo–X	Ct–Mo [a]	Ω	N–Mo–N	P–Mo–P	
2	[Mo(η^3-allyl)$(CO)_2$bipy$(NCCH_3)$]$^+$		2.232(3)	2.197(3)	2.035	94.8	72.6(1)		This work
5	[Mo(η^3-allyl)$(CO)_2$dppe$(NCCH_3)$]$^+$	2.570(4)		2.233(5)	2.096	90.8		78.2(1)	This work
6	[Mo(η^3-allyl)$(CO)_2$phenBr]		2.258(4)	2.645(2)	2.047	177.2	73.2(2)		This work
7	[Mo(η^3-allyl)$(CO)_2$bipyBr]		2.233(5)	2.650(3)	2.055	177.9	73.2(3)		This work
8	[Mo(η^3-allyl)$(CO)_2$dppeCl]	2.561		2.573	2.063	93.1		75.3	[7]
9	[Mo(η^3-allyl)$(CO)_2$bipy(NCS)]		2.186	2.117	2.019	175.9	73.0		[23b]
10	[Mo(η^3-allyl*)$(CO)_2$phen(NCS)] [b]		2.258	2.145	2.071	173.5	74.6		[26]
11	[Mo(η^3-allyl)$(CO)_2$bipy(pyr)]$^+$		2.250	2.321	2.047	174.9	71.1		[27]
12	[Mo(η^3-allyl)$(CO)_2$phen(CF_3COO)]		2.248	2.225	2.045	99.2	73.2		[28]
13	[{Mo(η^3-allyl)$(CO)_2$bipy}$_2$(μ-Cl)]$^+$		2.244	2.536	2.054	171.8	72.6		[4]

[a] Ct represents the centroid of the allyl ligand.
[b] η^3-allyl* is the η^3-methylallyl ligand.

most stable isomer the nitrogen atoms occupy two equatorial positions (A in Scheme 5). This difference, although small, explains that this isomer is found in the solid.

Both isomers present the most stable arrangement of the allyl group with the open face eclipsing the carbonyls. The distances and angles in the optimized structures are in good agreement with experimental ones, although a lengthening of around 0.08 Å is observed in all calculated Mo–N and Mo–C bonds. A pyramidalization of the allylic *anti* hydrogens characterized by H–C–C–C dihedral angles of around 40° (41 and 37° against 44 and 38° in the low temperature X-ray structure) has also been determined for both isomers and can be detected in Scheme 5.

A 180° rotation of the allyl ligand in **2** gives rise to a conformer 16 kJ mol^{-1} less stable for the equatorial isomer A, while an equivalent rotation in for the equatorial–axial complex B leads to an unstable structure, indicated by the fact that the convergence was not obtained.

A linear synchronous transit (LST) trigonal rotation path connecting the octahedral conformers A and B, through a trigonal prismatic arrangement of the ligands, was attempted (with frozen structural parameters) in order to estimate the activation barrier for their interconversion. The maximum was located for both trigonal prismatic conformations, with the highest barrier for the exchange of the chelating ligand from axial/equatorial to equatorial–axial (Fig. 8).

The shorter contacts between hydrogens of the bipyridyl and allyl groups in the trigonal prismatic arrangement may force the allyl to a η^1 geometry releasing some of the stereochemical stress and lowering the rotational barrier which is, according to our calculations, 270 kJ mol^{-1}. The same procedure was applied to the allyl rotation converting isomers A and A′ (Scheme 3). In the activated state, the central carbon atom is eclipsed with either a carbonylic carbon or a bipyridyl nitrogen. An extended Hückel analysis (Fig. 9) shows that the barrier to the free rotation of the allyl group may originate in the need to break the π interaction between the non-bonding π orbital and the Mo t_{2g} orbital of adequate symmetry.

Table 3
Hydrogen structural parameters of the allyl ligand at low temperature for **2**

Torsion angles (°)	
H(1A)–C(1)–C(2)–C(3)	−177(3)
H(1B)–C(1)–C(2)–C(3)	38(5)
H(3A)–C(3)–C(2)–C(1)	−44(4)
H(3B)–C(3)–C(2)–C(1)	170(4)
Dihedral angles (°)	
∠[C(1),C(2),C(3)]; [C(1), H(1A), H(1B)	34
∠[C(1),C(2),C(3)]; [C(3), H(3A), H(3B)	37
∠[C(1),C(2),C(3)]; [C(2), H(2)]	4
Distances of hydrogens to the allylic plane (Å)	
H(1A)	0.04(5)
H(1B)	−0.50(7)
H(2)	0.03(6)
H(3A)	−0.57(6)
H(3B)	0.14(5)

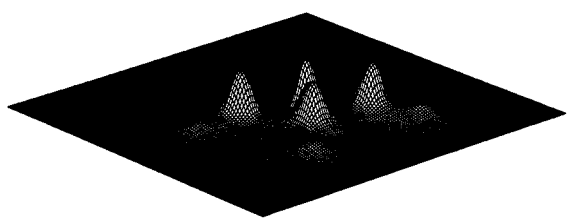

Fig. 7. Valence charge density map in the allylic plane of [Mo(η^3-allyl)$(CO)_2$bipy$(NCCH_3)$]PF_6 (**2**).

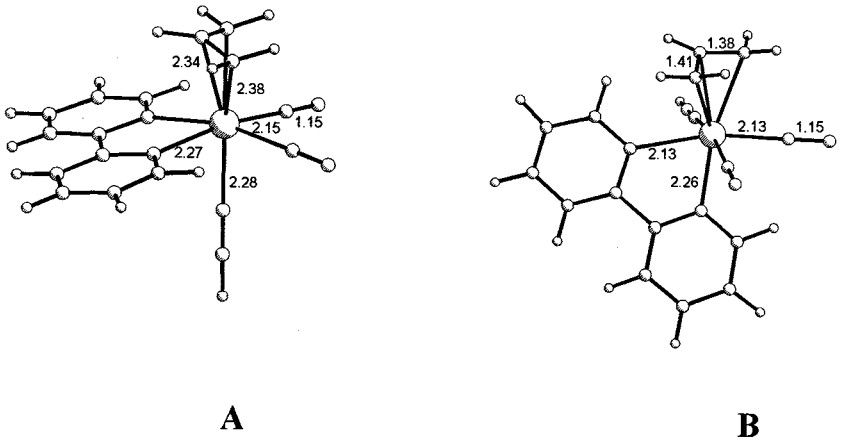

A **B**

Scheme 5.

3. Conclusions

The X-ray structures of the complexes [Mo(η^3-allyl)$(CO)_2L_2L']PF_6$ and [Mo(η^3-allyl)$(CO)_2L_2X$] studied showed the presence of either the equatorial or the equatorial–axial isomers, A and B in Scheme 1, respectively. The reasons determining these structural preference could not be established. Detailed dynamic NMR and ab initio studies were performed for complex **2**. Isomer A was found to predominate at room temperature and to be in equilibrium with another species (A′ in Scheme 3). These isomers differ by the coordination of the allyl group, eclipsing or not the carbonyl ligands, and have a small energy difference of 16 kJ mol^{-1}.

By lowering the temperature, another isomer was detected and assigned as B in Scheme 1. This species can be formed from A by a trigonal rotation mechanism, with a calculated barrier (HF) of 270 kJ mol^{-1}. The allyl group eclipses the carbonyl ligands in this isomer. Its rotation was not experimentally observed and the resulting (hypothetical) structure was found to be unstable from calculations.

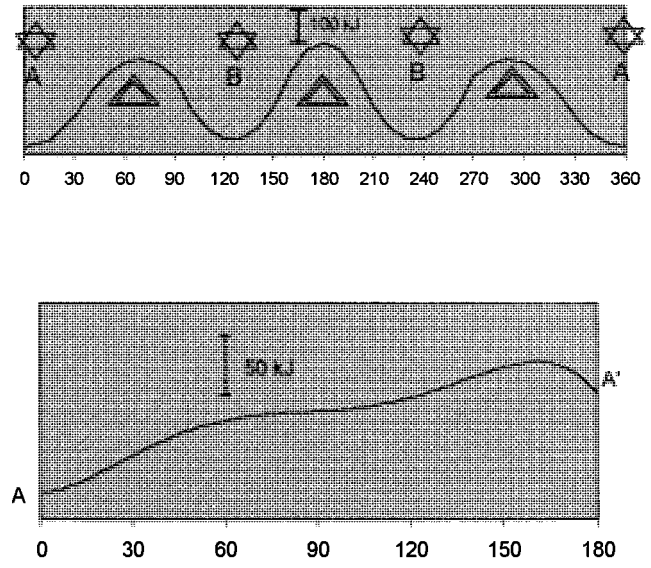

Fig. 8. LST energy plots for: (a) trigonal rotation of (L–L)L′ converting isomers A and B; (b) Mo-allyl rotation converting A and A′.

4. Experimental

4.1. Synthesis

All experiments were carried out under an atmosphere of argon by Schlenk techniques. Diethyl ether and pentane were dried by distillation from Na/benzophenone. Acetonitrile was dried over CaH_2 and distilled after refluxing several hours over CaH_2–P_2O_5. Dichlorometane was distilled from CaH_2. Acetone was distilled and kept over 4 Å molecular sieves.

[Mo(η^3-C_3H_5)$(CO)_2$bipyBr] [14], [Mo(η^3-C_3H_5)-$(CO)_2(CH_3CN)_2$Cl] [14], [Mo(η^3-C_3H_5)$(CO)_2py_2$Br][14],

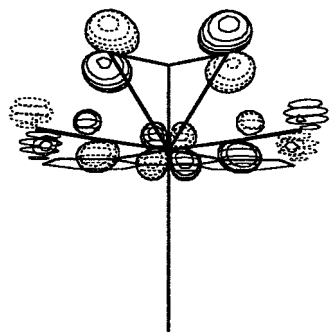

Fig. 9. Frontier orbital (EH) of [Mo(η^3-allyl)$(CO)_2$bipy$(NCCH_3)$]$^+$ (**2**) depicting the interaction between a non bonding π orbital of the allyl group and a t_{2g} metal centered orbital of appropriate symmetry.

[Mo(η^3-C_3H_5)(CO)$_2$phenBr] [14] and $PhSCH_2CH_2SPh$ [30] were prepared as described.

4.2. Analytical procedures

Microanalysis were performed in the analytical laboratory of Instituto Superior Técnico. Proton and carbon NMR spectra were obtained with a Bruker CXP 300 spectrometer and a Varian Unit 300. Phase sensitive NOESY spectra were obtained with a mixing time of 0.6 s at 27 and −30 °C. Infrared spectra were recorded on a Perkin–Elmer 457 spectrophotometer using KBr pellets.

4.2.1. Preparation of [Mo(η^3-C_3H_5)(CO)$_2$-($PhSCH_2CH_2SPh$)]PF_6 (1)

A solution of $PhSCH_2CH_2SPh$ (0.135 g, 0.53 mmol) in acetone (5 ml) was added to a solution of [Mo(η^3-C_3H_5)(CO)$_2$($NCCH_3$)Cl] (0.166 g, 0.53 mmol) in the same solvent (10 ml). After 3 h stirring and evaporation to dryness, the residue was washed with pentane at −70 °C to give a yellow powder in 50% yield (0.157 g). The product is an oil at RT and it should be stored under −20 °C.

^{1}H-NMR spectrum (d_6-acetone, 253 K), δ (ppm): 7.19, −7.41 (m, 10H, C_6H_5); 3.66 (m, 1H, H_{meso}); 3.33 (d, 2H, [$^3J(^1H-^1H_{meso}) = 5.9$ Hz], H_{syn}); 3.12 (s, 4H, SCH_2CH_2S); 0.81 (d, 2H, [$^3J(^1H-^1H_{meso}) = 10.3$ Hz, [$^2J(^1H-^1H_{syn}) = 2.9$ Hz], H_{anti}).

4.2.2. Preparation of [Mo(η^3-C_3H_5)(CO)$_2$(-$NCCH_3$)bipy]PF_6 (2)

A suspension of [Mo(η^3-C_3H_5)(CO)$_2$bipyBr] (1.25 g, 2.93 mmol) in 40 ml of CH_3CN was treated with excess $TlPF_6$ (1.23 g, 3.52 mmol). After refluxing for 3 h, the resulting red solution was filtered several times and evaporated to dryness. The compound was obtained as red crystals by diffusion of Et_2O in a solution of acetonitrile. Yield, 80% (1.340 g). Anal. Found: C, 37.9; H, 3.2; N, 7.9. Calc. for $C_{20}H_{16}F_6MoN_3O_2P$: C, 38.2; H, 3.0; N, 7.9%.

IR (KBr, RT): 3100–3040, 2280, 1940, 1600, 1470, 1440, 830, 760, 550. ^{1}H-NMR spectrum (CD_3CN, 300K), δ (ppm): Isom. A, 7.62–8.86 (m, 8H, *bipy*); 4.08 (tt, [$^3J(^1H-^1H_{anti}) = 9.4$ Hz, $^3J(^1H-^1H_{syn}) = 6.5$ Hz], 1H, H_{meso}); 3.45 (d, 2H, [$^3J(^1H-^1H_{meso}) = 6.5$ Hz], H_{syn}); 1.95 (s, 3H, NCCH_3); 1.58 (d, 2H, [$^3J(^1H-^1H_{meso}) = 9.8$ Hz], H_{anti}). Isom. A′, 7.62–8.86 (m, 8H, *bipy*); 3.63 (d, 2H, [$^3J(^1H-^1H_{meso}) = 6.1$ Hz], H_{syn}); 3.24 (tt, [$^3J(^1H-^1H_{anti}) = 9.4$ Hz, $^3J(^1H-^1H_{syn}) = 6.5$ Hz], 1H, H_{meso}); 1.95 (s, 3H, NCCH_3); 1.65 (d, 2H, [$^3J(^1H-^1H_{meso}) = 9.8$ Hz], H_{anti}). ^{13}C-NMR spectrum (CD_3CN, 300 K), δ (ppm): isom. A and A′, 223.4, 223.2 (2*C*O); 154.1, 153.5, 152.8, 152.4, 140.3, 127.3, 127.1 (*bipy*); 123.6 (CH_3CN); 74.4, 72.1 (C_{meso}); 59.4, 59.0 (C_{term}). ^{1}H-NMR spectrum (CD_3CN, 335 K), δ (ppm): 7.73–8.38 (m, 8H, *bipy*); 3.57 (br, 2H, H_{syn}); 1.62 (d, 2H, H_{anti}). ^{13}C-NMR spectrum (CD_3CN, 335 K), δ (ppm): 223.2 (*C*O); 153.7, 152.5, 140.3, 127.2 (*bipy*); 123.6 (CH3*C*N); 72.6 (C_{meso}); 59.2 (C_{term}). ^{1}H-NMR spectrum (CD_3CN, 223 K), δ (ppm): Isom. A, 7.65–8.90 (m, 8H, *bipy*); 4.08 (tt, [$^3J(^1H-^1H_{anti}) = 9.4$ Hz, $^3J(^1H-^1H_{syn}) = 6.5$ Hz], 1H, H_{meso}); 3.44 (d, 2H, [$^3J(^1H-^1H_{meso}) = 6.1$ Hz], H_{syn}); 1.95 (s, 3H, NCCH_3); 1.67 (d, 2H, [$^3J(^1H-^1H_{meso}) = 9.8$ Hz], H_{anti}). Isom. B, 7.65–8.90 (m, 8H, *bipy*); 3.81 (br, 1H, H_{syn}); 3.45 (br, 1H, H_{syn}); 3.27 (tt, [$^3J(^1H-^1H_{anti}) = 9.4$ Hz, $^3J(^1H-^1H_{syn}) =$ 6.2 Hz], 1H, H_{meso}); 1.95 (s, 3H, NCCH_3); 1.67 (br, 1H, H_{anti}); 1.52 (br, 1H, H_{anti}). ^{13}C-NMR spectrum (CD_3CN, 223 K), δ (ppm): Isom. A, 223.6 (*C*O); 154.0, 153.0, 140.3, 127.1 (*bipy*); 123.5 (CH_3CN); 73.8 (C_{meso}); 59.0 (C_{term}). Isom. B, 222.4, 222.2 (2 *C*O); 154.9, 152.6, 140.8, 139.8, 131.2, 127.7, (*bipy*); 123.8 (CH_3CN); 71.7 (C_{meso}); 61.8, 56.9 (C_{term}).

4.2.3. Preparation of [Mo(η^3-C_3H_5)(CO)$_2$-($NCCH_3$)$_2$py]PF_6 (3)

[Mo(η^3-C_3H_5)(CO)$_2$pyBr] (0.573 g, 1.33 mmol) was suspended in 25 ml of CH_3CN and treated with $TlPF_6$ (0.512 g, 1.46 mmol). After refluxing for 2 h, TlBr was filtered off and the solution obtained was taken to dryness. The residue was repeatedly washed with pentane. A yellow compound was obtained in 70% yield (0.465 g) after recrystallization from CH_2Cl_2–pentane. Anal. Found: C, 33.5; H, 3.2: N, 7.8. Calc. for $C_{14}H_{16}F_6MoN_3O_2P$: C, 33.7; H, 3.2; N, 8.4%.

IR (KBr, RT): 3080, 3010, 2280, 1950, 1600, 1485, 1440, 830, 750, 550. ^{1}H-NMR spectrum (CD_3CN, 300K), δ (ppm): Isom. A, A′ and B, 7.43–8.66 (m, 15H, *py*); 4.12 (m, 3H, H_{meso}); 3.65 (br, 4H, H_{syn}); 3.57 (d, 2H, [$^3J(^1H-^1H_{meso}) = 6.5$ Hz], H_{syn}); 2.33 (s, 18H, CH_3CN); 1.77 (d, 2H, [$^3J(^1H-^1H_{meso}) = 9.8$ Hz], H_{anti}); 1.46 (d, 2H, [$^3J(^1H-^1H_{meso}) = 10.2$ Hz], H_{anti}).

4.2.4. Preparation of [Mo(η^3-C_3H_5)(CO)$_2$($NCCH_3$)$_3$]PF_6 (4)

$TlPF_6$ (1.70 g, 4.87 mmol) was added to a solution of [Mo(η^3-C_3H_5)(CO)$_2$($NCCH_3$)$_2$Cl] (1.25 g, 4.03 mmol) in 40 ml CH_3CN. After refluxing for 3 h, TlCl was filtered off and the yellow solution obtained was taken to dryness. The residue was repeatedly washed with Et_2O (2 × 5 ml). Orange crystals were obtained in 70% yield (1.572 g) after recrystallization from CH_2Cl_2/pentane. Anal. Found: C, 28.9; H, 3.2; N, 9.1. Calc. for $C_{11}H_{14}F_6MoN_3O_2P$: C, 28.6; H, 3.0; N, 9.1%.

IR (KBr, RT): 3060, 2290, 1955, 1865, 830, 550. ^{1}H-NMR spectrum ($CDCl_3$, 300 K), δ (ppm): 3.89 (m, 1H, H_{meso}); 3.44 (d, 2H, [$^3J(^1H-^1H_{meso}) = 6.3$ Hz], H_{syn}); 2.38 (br, 9H, CH_3CN); 1.42 (d, 2H, [$^3J(^1H-^1H_{meso}) = 9.7$ Hz], H_{anti}).

Table 4
Crystallographic data and pertinent structure refinement details for complexes **2**, **5**, **6** and **7**

	2	**5**	**6**	**7**
Empirical formula	$C_{17}H_{16}F_6MoN_3O_2P$	$C_{31}H_{32}F_6MoNO_4P_3$	$C_{17}H_{12}BrMoN_2O_2$	$C_{15}H_{13}BrMo_2N_2O_2$
Formula weight	535.24	785.43	452.14	429.12
Crystal system	Monoclinic	Triclinic	Monoclinic	Monoclinic
Space group	$P2_1/n$	$P\bar{1}$	$P2_1/c$	$P2_1/m$
Unit cell dimensions				
a (Å)	8.088(2)	9.850(13)	9.722(14)	7.032(14)
b (Å)	20.083(5)	11.408(16)	12.244(17)	13.792(20)
c (Å)	12.682(2)	16.848(21)	14.249(19)	8.185(12)
α (°)		76.18(1)		
β (°)	100.16(2)	81.85(1)	102.91(1)	100.64(1)
γ (°)		67.32(1)		
V (Å^3)	2028	1694	1653	780
Z	4	2	4	2
D_{calc} (Mg m^{-3})	1.753	1.540	1.816	1.827
$F(000)$	1064	796	884	420
Absorption coefficient (mm^{-1})	0.799	0.598	3.220	3.406
θ Range (°)	1.92–31.96	1.98–25.96	2.22–25.96	2.53–26.11
Index ranges hkl	$-11\leq h\leq 11$, $-29\leq k\leq 27$, $-18\leq l\leq 18$	$0\leq h\leq 12$, $-12\leq k\leq 13$, $-20\leq l\leq 20$	$-11\leq h\leq 0$, $-14\leq k\leq 15$, $-17\leq l\leq 17$	$0\leq h\leq 8$, $-16\leq k\leq 16$, $-10\leq l\leq 9$
Reflections collected	8036	6031	5520	2718
Unique reflections (R_{int})	6428 (0.0250)	6031	3121 (0.0301)	1584 (0.0539)
Data/restraints/parameters	6037/0/335	6031/5/429	3121/1/220	1584/0/101
Goodness-of-fit on F^2	1.155	1.081	1.109	1.128
Final R indices [$I>2\sigma(I)$], R_1 and wR_2	0.0577, 0.1768	0.0582, 0.1483	0.0439, 0.1117	0.0459, 0.1098
R indices (all data), R_1 and wR_2	0.0675, 0.1995	0.0878, 0.1632	0.0599, 0.1202	0.0671, 0.1227
Largest difference peak and hole (e Å^{-3})	1.971, −2.741	0.845, −0.905	0.867, −0.837	1.316, −0.573

*4.2.5. Preparation of [Mo(η^3-C$_3$H$_5$)(CO)$_2$-(NCCH$_3$)dppe]PF$_6$ (**5**)*

$[Mo(\eta^3\text{-}C_3H_5)(CO)_2(NCCH_3)_3]PF_6$ (0.323 g, 0.70 mmol) was dissolved in 50 ml of CH_2Cl_2 and treated with one equivalent gram of dppe (0.28 g, 0.70 mmol). The reaction mixture was stirred for 2 h. The solvent was removed in vacuo. The residue was recrystallized from CH_2Cl_2/pentane to give an orange compound in 74% yield (0.403 g). Anal. Found: C, 50.2; H, 4.4; N, 2.1. Calc. for $C_7H_8F_6MoNO_2P$: C, 51.0; H, 4.1; N, 1.8%.

IR (KBr, RT): 3040, 2300, 2280, 1950, 1475, 1430, 830, 750, 700, 550. ^{1}H-NMR spectrum (acetone-d^6, 300 K), δ (ppm): 7.17–7.98 (m, 20H, C_6H_5); 4.62 (tt, [$^3J(^1H-^1H_{anti}) = 11.4$ Hz, $^3J(^1H-^1H_{syn}) = 6.9$ Hz], 1H, H_{meso}); 4.02 (d, 2H, [$^3J(^1H-^1H_{meso}) = 7.2$ Hz], H_{syn}); 3.09 (m, 2H, PCH_2CH_2P); 2.81 (m, 2H, PCH_2CH_2P); 2.27 (d, 2H, [$^3J(^1H-^1H_{meso}) = 11.4$ Hz], H_{anti}); 1.80 (s, 3H, $NCCH_3$). ^{13}C-NMR spectrum (acetone-d^6, 300 K), δ (ppm): 222.9 (*C*O); 116.1–132.4 (C_6H_5); 93.6 (C_{meso}); 61.0 (C_{term}); 26.5 (CH_2, dppe); 1.9 (CH_3CN). ^{31}P{^{1}H}-NMR spectrum (acetone-d^6, 300 K), δ (ppm): 63.62. ^{31}P{^{1}H}-NMR spectrum (CD_2Cl_2, 183 K), δ (ppm): Isom. A and A′: 68.75 (br), 66.29 (br). Isom. B: 52.0 (d, 2P, $J(^{31}P-^{31}P) = 54$ Hz; 52.3 (d, 2P, $J(^{31}P-^{31}P) = 54$ Hz).

4.3. Crystallography

Crystallographic data are summarized in Table 4 together with data collection parameters and pertinent refinement details for complexes **2**, **5**, **6** and **7**. Crystal data of **2** were measured at room and low temperatures, while the data of the remaining three complexes were collected only at room temperature.

The room temperature data were collected with a MAR research Image Plate system using graphite-monochromated Mo–K_α radiation at the University of Reading. The crystals were positioned at 70 mm from the image plate. Ninety-five frames were measured at 2° intervals with counting time adequate to the diffraction pattern exhibited by the crystal under investigation. Data analysis was carried out with the XDS program [31]. An empirical absorption correction using a version of DIFABS [32] modified for image plate geometry, was applied to the intensities of the complexes **6** and **7**, respectively. Low temperature data for complex **2** were collected at the Instituto Tecnológico e Nuclear on an Enraf–Nonius CAD4 equipped with a FR558NH nitrogen flow cryostat and Mo–K_α radiation. Data reduction, Lorentz polarization, decay and analytical absorption corrections were carried out with REFPK, BGLP, SCALE3 and ABL programs [33].

All structures were solved by direct methods with SHELXS [34]. The hydrogen atoms were inserted in the refinement in geometric idealized positions apart from allylic ones of **2**, **5** and **6**, which were localized form difference Fourier maps. All non-hydrogen atoms were refined with anisotropic thermal displacements. All hydrogen atoms were refined giving isotropic thermal parameters equivalents to 1.2 times that of the carbon atom to which they were bonded, except the allylic hydrogens of the X-ray determination of **2** at low temperature, which were refined with individual isotropic thermal parameters. The structures were then refined by full matrix least-squares methods on F^2 with SHELXL [35] using the weighting scheme with standard form until the convergence is achieved. The ORTEP molecular diagrams presented were drawn with PLATON [36] and ZORTEP [37] graphical softwares.

4.4. Calculations

Combined ab initio [22] and extended Hückel [21] calculations were carried out on model complexes. Ab initio calculations were performed at DFT level with a B3LYP/3-21G* basis set using the GAUSSIAN94/DFT program [22]. Extended Hückel type calculations with modified H_{ij} were also carried out [38]. The basis set for the metal atom consisted of ns, np and $(n-1)$d-orbitals. The s and p were described by single Slater type wavefunctions, and d-orbitals were taken as contracted linear combinations of two Slater type wavefunctions. Standard parameters were used for all atoms. The EHMO calculations and drawings were made with CACAO [39]. In all ab initio calculations the methyl group of NCMe was modeled by a hydrogen atom.

5. Supplementary material

Crystallographic data for the structural analysis have been deposited with the Cambridge Crystallographic Data Center, CCDC Nos. 159344 (low temperature) and 159345 (room temperature) for **2**, 159346 for **5**, 159347 for **6** and 159348 for **7**. Copies of this information may be obtained free of charge from The Director, CCDC, 12 Union Road, Cambridge CB2 1EZ, UK [fax: +44-1223-336033; e-mail: deposit@aadc.cam.ac.uk or www: http://www.ccdc.cam.ac.uk].

Acknowledgements

MJC and PC thank the TMR Transition Metal Clusters in Catalysis and Organic Synthesis. VF acknowledges FCT and the British Council for funding. The University of Reading and EPSRC are thanked for funds for the Image Plate system.

References

[1] P.K. Baker, Adv. Organomet. Chem. 40 (1996) 45.
[2] (a) F. Dewans, J. Dewailly, J. Meunier-Piret, P. Piret, J. Organomet. Chem. 76 (1974) 53;
(b) F. Dewans, E. Goldenberg, Brevet d'Invention, Inst. Int. Prop. Indust. (1972) 2.120.573.
[3] (a) B.M. Trost, M.J. Lautens, Organometallics 2 (1983) 1687;
(b) B.M. Trost, M.J. Lautens, J. Am. Chem. Soc. 104 (1982) 5543;
(c) B.M. Trost, M.J. Lautens, J. Am. Chem. Soc. 105 (1982) 3343;
(d) B.M. Trost, M.-H. Hung, J. Am. Chem. Soc. 105 (1983) 7757;
(e) B.M. Trost, M.-H. Hung, J. Am. Chem. Soc. 106 (1984) 6837;
(f) M.P.T. Sjögren, H. Frisell, B. Åkermark, P. -O. Norrby, L. Eriksson, A. Vitagliano, Organometallics 16 (1997) 942.
[4] (a) M.D. Curtis, O. Eisenstein, Organometallics 3 (1984) 887;
(b) M.D. Curtis, N.A. Fotinos, J. Organomet. Chem. 272 (1984) 43.
[5] P. Espinet, R. Hernando, G. Iturbe, F. Villafañe, A.G. Orpen, I. Pascual, Eur. J. Inorg. Chem. (2000) 1031.
[6] (a) B.J. Brisdon, K.E. Paddick, J. Organomet. Chem. 149 (1978) 113;
(b) B.J. Brisdon, A.A. Wolf, J. Chem. Soc. Dalton Trans. (1978) 291;
(c) J.W. Faller, D.A. Haitko, R.D. Adams, D.F. Chodosh, J. Am. Chem. Soc. 99 (1978) 1654;
(d) J.W. Faller, D.H. Haitko, J. Organomet. Chem. 149 (1978) C19;
(e) B.J. Brisdon, M. Cartwright, J. Organomet. Chem. 164 (1979) 83.
[7] J.W. Faller, D.A. Haitko, R.D. Adams, D.F. Chodosh, J. Am. Chem. Soc. 101 (1979) 865.
[8] (a) B.J. Brisdon, M. Cartwright, A.G. Hodson, J. Organomet. Chem. 227 (1984) 85;
(b) B.J. Brisdon, M. Cartwright, A.G. Hodson, M.F. Mahon, K.C. Molloy, J. Organomet. Chem. 435 (1992) 319.
[9] C. Borgmann, C. Limberg, L. Zsolnai, K. Heinze, Z. Naturforsch. Teil b 54 (1999) 473.
[10] (a) D.S. Frohnapfel, P.S. White, J.L. Templeton, H. Rüegger, P.S. Pregosin, Organometallics 16 (1997) 3737;
(b) S.K. Chowdhury, M. Nandi, U.S. Joshi, A. Sarkar, Organometallics 16 (1997) 1806;
(c) K.-B. Shiu, C.-J. Chang, Y. Wang, M.-C. Cheng, J. Organomet. Chem. 406 (1991) 363.
[11] J.A. Casares, P. Espinet, Inorg. Chem. 36 (1997) 5428.
[12] W.J. Faller, M.J. DiVerdi, J.A. John, Tetrehedron Lett. 32 (1991) 1271.
[13] Y.D. Ward, A. Villaneuva, J. Allred, C.P. Sonha, M.A. Semones, L.S. Liebeskind, Organometallics 14 (1995) 4132.
[14] H. tom Dieck, H. Friedel, J. Organomet. Chem. 14 (1968) 375.
[15] (a) S. Trofimenko, J. Am. Chem. Soc. 90 (1968) 4754;
(b) S. Trofimenko, J. Am. Chem. Soc. 91 (1969) 3183;
(c) S. Trofimenko, Inorg. Chem. 9 (1970) 2493.
[16] (a) A.T.T. Hsieh, B.O. West, J. Organomet. Chem. 112 (1976) 285;
(b) A.T.T. Hsieh, B.O. West, J. Organomet. Chem. 78 (1974) C40.
[17] B.J. Brisdon, J. Organomet. Chem. 125 (1977) 225.
[18] (a) R.G. Hayter, J. Organomet. Chem. 13 (1968) P1;
(b) J.W. Faller, C. Chen, M.J. Mattine, A. Jakubowski, J. Organomet. Chem. 52 (1973) 361.
[19] B.J. Brisdon, G.F. Griffin, J. Chem. Soc. Dalton Trans. (1975) 1999.

[20] M.F. Perpinan, A. Santos, J. Organomet. Chem. 218 (1981) 185.
[21] (a) R. Hoffmann, W.N. Lipscomb, J. Chem. Phys. 36 (1962) 2872;
(b) R. Hoffmann, W.N. Lipscomb, J. Chem. Phys. 37 (1962) 3489.
[22] M.J. Frisch, G.W. Trucks, H.B. Schlegel, P.M.W. Gill, B.G. Johnson, M.A. Robb, J.R. Cheeseman, T. Keith, G.A. Petersson, J.A. Montgomery, K. Raghavachari, M.A. Al-Laham, V.G. Zakrzewski, J.V. Ortiz, J.B. Foresman, J. Cioslowski, B.B. Stefanov, A. Nanayakkara, M. Challacombe, C.Y. Peng, P.Y. Ayala, W. Chen, M.W. Wong, J.L. Andres, E.S. Replogle, R. Gomperts, R.L. Martin, D.J. Fox, J.S. Binkley, D.J. Defrees, J. Baker, J.P. Stewart, M. Head-Gordon, C. Gonzalez, and J.A. Pople, Gaussian 94, Revision C.3, Gaussian, Inc., Pittsburgh PA, 1995.
[23] (a) B.J. Brisdon, M. Cartwright, J. Organomet. Chem. 128 (1977) C15;
(b) A.J. Graham, R.H. Fenn, J. Organomet. Chem. 17 (1969) 405.
[24] P. Powell, J. Organomet. Chem. 129 (1975) 175.
[25] C.G. Hull, M.H.B. Stiddard, J. Organomet. Chem. 9 (1967) 519.
[26] A.J. Graham, R.H. Fenn, J. Organomet. Chem. 25 (1970) 173.
[27] R.H. Fenn, A.J. Graham, J. Organomet. Chem. 37 (1972) 137.
[28] L. Eriksson, M.P.T. Sjogren, B. Akermark, Acta Crystallogr. Sect. C 52 (1996) 77.
[29] F.H. Allen, J.E. Davies, J.J. Galloy, O. Johnson, O. Kennard, C.F. Macrae, E.M. Mitchell, G.F. Mitchel, J.M. Smith, D.G. Watson, J. Chem. Inf. Comp. Sci. 31 (1991) 187.
[30] F.R. Hartley, S.G. Murray, W. Levason, H.E. Soutter, C.A. McAuliffe, Inorg. Chim. Acta 35 (1979) 265.
[31] W. Kabsch, J. Appl. Crystallogr. 21 (1988) 916.
[32] N. Walker, D. Stuart, Acta Crystallogr. Sect. A 39 (1983) 158.
[33] R.H. Blessing, Data Reduction and Error Analysis for Accurate Single Crystal Diffraction Intensities, Medical Foundation of Buffalo, USA.
[34] G.M. Sheldrick, Acta Crystallogr. Sect. A 46 (1990) 467.
[35] G.M. Sheldrick, SHELX-97, University of Göttingen, 1997.
[36] A.L. Spek, PLATON, A Multipurpose Crystallographic Tool, Utrecht University, Utrecht, The Netherlands, 1999.
[37] L. Zsolnai, XPMA and ZORTEP, University of Heidelberg, 1994.
[38] J.H. Ammeter, H.-B. Bürgi, J.C. Thibeault, R. Hoffmann, J. Am. Chem. Soc. 100 (1978) 3686.
[39] C. Mealli, D.M. Proserpio, J. Chem. Educ. 67 (1990) 399.